Molecular Dynamics Studies on the Condensation Coefficient of Water

Takaharu Tsuruta and Gyoko Nagayama*

Department of Mechanical Engineering, Kyushu Institute of Technology, Sensui-cho 1-1, Tobata, Kitakyushu 804-8550, and Department of Mechanical and Electrical Engineering, Tokuyama College of Technology, 3538 Takajo, Kume, Shunan, Yamaguchi 745-8585, Japan

Received: July 1, 2003; In Final Form: November 20, 2003

Molecular dynamics (MD) simulations are carried out for water using two kinds of intermolecular potentials, the Carravetta−Clementi (C−C) model and the extended simple point charge (SPC/E) model, to understand the mechanism of interface mass transfer between liquid and vapor. Effects of different interface structures on the condensation process are investigated, and computational data on the condensation coefficient are presented. By changing incident conditions such as the translational and rotational energies of the incident molecules on the liquid surface, we find that the condensation coefficient of water primarily depends on the translational energy and the surface temperature, as is the case for a simple gas such as argon. The molecular exchange phenomenon caused by incident molecules has no marked influence on the condensation coefficient. A formula for the condensation coefficient is summarized as a function of the surface-normal component of the translational energy and the surface temperature. Also, relations between the surface structure and the condensation coefficient are discussed based on the transition state theory developed in our previous study. The paper demonstrates that the theory can explain the MD data very well, and it is concluded that the translational motion is important compared with the rotational motion, even for polyatomic molecules.

I. Introduction

In the expression of the interface mass transfer rate, the condensation coefficient, that is, the possibility that an incident vapor molecule may condense into the liquid phase, is an unknown factor, but it plays an important role as a property of the substance. Although a great deal of effort has been made with experimental and theoretical studies for a considerable length of time, there is little agreement upon the data. Especially for water, numerous experimental data are available. They are widely scattered, and no evidence has been shown that the condensation coefficient is a constant property.[1−3] For example, values very close to unity have been reported by Mills and Seban,[4] Maa,[5] and Wenzel,[6] whereas values less than unity have been obtained by Bonacci et al.,[7] Tanaka and Hatamiya,[8] Fujikawa and Maerefat,[9,] Maerefat et al.[10] and Tsuruta et al.[11] Table 1 summarizes these published data in brief. To explain the small value of the condensation coefficient, a theoretical expression has been presented by Fujikawa and Maerefat[9] based on transition state theory.[12] They assumed that the condensation coefficient of polyatomic vapor is significantly smaller than unity because of the constraint of molecular rotational motion in the liquid state. Their theoretical predictions for water at 300 K range from 0.3 to 0.4, which agree well with those measured in a dropwise condensation experiment by Hatamiya and Tanaka.[8] Later, Matsumoto and co-workers published a new explanation for the small value of the condensation coefficient based on their molecular dynamics (MD) simulations.[13−20] They suggest that molecular exchange like a "spattering" phenomenon caused by collisions of vapor molecules with the liquid surface significantly reduces the condensation coefficients for polyatomic molecules. Thus, Fujikawa and Matsumoto agree about the small value of the condensation coefficients,[21,22] and a "hot spot" model has been suggested by Chekmarev[23] to support the consideration of the molecular exchange phenomenon. However, most recently Meland pointed out an error in the paper of Matsumoto and co-workers, and he argued that molecular exchange has no influence on gas-kinetic calculations of phase change.[24]

TABLE 1: Experimental Data for the Condensation Coefficients of Water

author(s)	$\bar{\sigma}_c$	temp (K)
Mills and Seban[4]	0.450−1.000	281−283
Maa[5]	1.000	274−281
Wenzel[6]	1.000	295−319
Bonacci et al.[7]	0.417−0.693	279−280
Hatamiya and Tanaka[8]	0.380−0.510	280
	0.330−0.480	300
Fujikawa et al.[9]	0.270−0.430	297
Maerefat et al.[10]	0.100−0.350	297−299
Tsuruta et al.[11]	0.400−0.680	280
	0.350−0.700	300

Recent molecular dynamics studies on the condensation and evaporation of monatomic argon reveal that the condensation/evaporation coefficient is not uniform but a function of the surface-normal component of the translational energy for vapor molecules.[25−27] This indicates the necessity of considering the effects of molecular kinetics on the interface mass transfer rate. It is reported that the molecular boundary conditions of condensation, evaporation, and reflection have a dramatic effect on the evaluation of the temperature jump at the liquid−vapor interface.[28−30] By considering the translational motion as a primary factor in the condensation, we have proposed a new theoretical expression of the condensation coefficient based on transition state theory which gives a good explanation for the MD results.[31,32] However, for polyatomic molecules there is still no conclusive proof of the effect of molecular motion including

* Author to whom correspondence should be addressed. E-mail: nagayama@tokuyama.ac.jp.

10.1021/jp035885q CCC: $27.50
Published on Web 01/07/2004

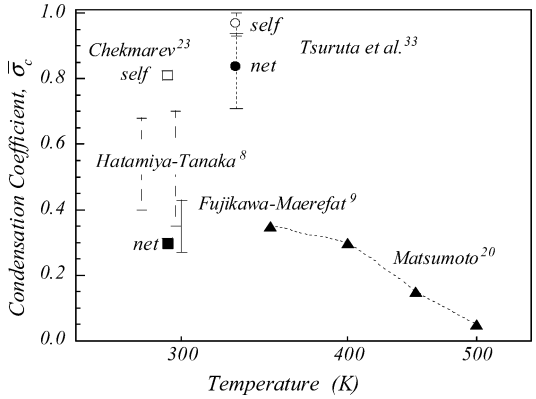

Figure 1. Recent data on the condensation coefficient of water. All symbols linked with dotted lines are from MD simulations: circles (open, self; filled, net) correspond to Tsuruta et al.[34] and triangles (net) to Matsumoto.[20] Experimental values from Hatamiya and Tanaka[8] are represented by broken lines and values from Fujikawa and Maerefat[9] are represented by the solid line. The open square (self) and the filled square (net) are theoretical predictions by Chekmarev[23] based on the "hot spot" model.

rotation on the condensation probability. Additionally, the complications of the molecular exchange for the associating liquids make it difficult to handle its effect on the condensation coefficient correctly. If molecular exchange plays an important role in reducing the condensation coefficient, the reason for its occurrence should be investigated. An earlier attempt using molecular dynamics simulation based on the Carravetta−Clementi (C−C)[33] potential model for water has been made to examine the occurrence of molecular exchange.[34] The simulations indicated that the incident molecules sometimes cause emissions of surface molecules, and this brings about the molecular exchange between condensation and evaporation molecules. However, the occurrence is infrequent, and as shown in Figure 1, there is no marked effect on the net value of the condensation coefficient. Figure 1 also shows some of the recent published data on the condensation coefficients of water.

Considering the situations mentioned above, further research from a microscopic point of view is needed to reveal the mechanism of the condensation process and the molecular exchange effect. Especially, the condensation coefficient of water should be fully investigated owing to its practical importance. Therefore, we focus on water in this paper and investigate the effects of the motion of polyatomic molecules on the condensation coefficient. Through the application of two kinds of water potential models, our paper is able to provide an examination of how the interface structure affects the calculations of condensation coefficients. The effects of molecular exchange on the condensation coefficient at different interface structures are studied first. The interactions of the incident molecules with the liquid surface molecules are examined by conducting 100 sample injections for each mode of molecular incident motion. Then, the condensation coefficients are obtained by counting the condensing molecules at different surface temperatures, and the dependency of the condensation coefficient on the incident kinetic energy is analyzed. Finally, the liquid−vapor interface structure is examined, and comparisons of the computational data with the theoretical results are made.

II. Background

In the ordinary expressions of the interface mass transfer rate, the condensation coefficient has been considered to have a

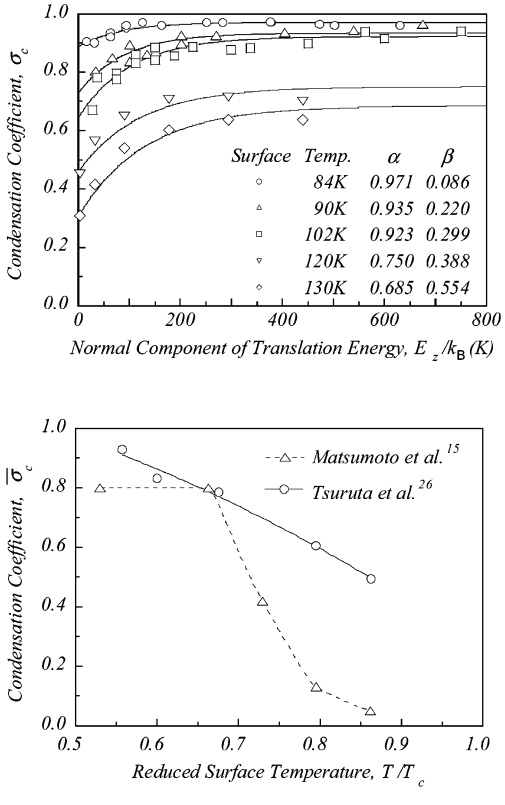

Figure 2. Condensation coefficients of monatomic argon. All symbols correspond to the MD data. (a) Dependency of the condensation coefficients on the normal component of translational energy at different temperatures. The solid lines correspond to eq 1 with the parameters α and β listed. (b) Dependence of the average condensation coefficients on surface temperature. The temperature is reduced by the critical temperature of argon, $T_c = 150.86$ K, and the lines are guides for the eye.

uniform value irrespective of the motion of molecules. It corresponds to the mean condensation probability for all incoming vapor molecules at the liquid−vapor interface. Previous molecular dynamics studies[25−27] show that the condensation coefficient of monatomic argon depends on the translational motion. Before discussing the condensation behavior of water vapor, we shall summarize the results obtained from the argon system.

Figure 2 shows the condensation coefficients of argon at different surface temperatures ranging from 84 to 130 K. The condensation coefficient σ_c is defined as the fraction of incident molecules that condense at the liquid surface, and the surface temperature is equal to the liquid phase temperature. The condensation coefficients are plotted in Figure 2a as a function of the surface-normal component of the translational energy E_z of the incident vapor molecules. Although the condensation coefficient for the surface at the triple point is close to unity, an increase in the surface temperature reduces the condensation coefficient, and the decrease is significant for the smaller incident energy. This indicates that high-energy molecules condense easily to the interface. Considering these behaviors, the following new formulation has been proposed for the condensation coefficient σ_c for each incident molecule:

$$\sigma_c = \alpha\left[1 - \beta \exp\left(-\frac{E_z}{k_B T}\right)\right] \quad (1a)$$

$$E_z = \frac{1}{2} m V_z^2 \quad (1b)$$

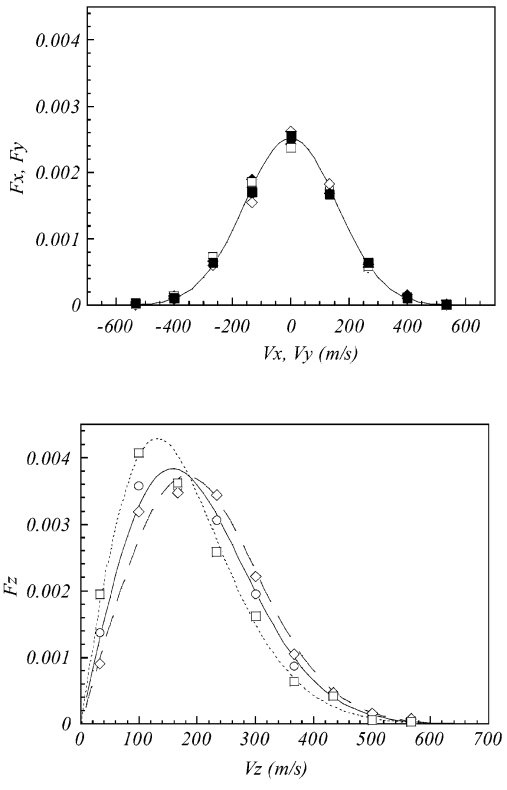

Figure 3. Boundary conditions for all-leaving, evaporated, and reflected molecules at the liquid−vapor interface of argon at 120 K. Circles are for all-leaving molecules, diamonds are for evaporated molecules, squares are for reflected molecules, and the solid line represents the Maxwellian velocity distribution. (a) Velocity distribution density functions for the tangential components. Open symbols correspond to the *x*-component and filled symbols to the *y*-component. (b) Velocity distribution density functions for the surface-normal component. The broken line is for eq 3a and the dotted line is for eq 3b.

where α and β are constants shown in Figure 2a, k_B is the Boltzmann constant, T is the surface temperature, m is the mass of a molecule, and V_z is the molecular velocity component perpendicular to the interface. Because the ordinary condensation coefficient $\bar{\sigma}_c$ is a macroscopic parameter related to the average behavior of an ensemble, it is equivalent to the integral-averaging result of eq 1 by applying a Maxwellian ensemble under equilibrium conditions. That is,

$$\bar{\sigma}_c = \frac{1}{(k_B T/2\pi m)^{1/2}} \int_0^\infty \sigma_c V_z \left(\frac{m}{2\pi k_B T}\right)^{1/2} \exp\left(-\frac{mV_z^2}{2k_B T}\right) dV_z = \alpha(1-\beta/2) \quad (2)$$

Figure 2b shows the results of eq 2, and it is clear that the ordinary condensation coefficient decreases with an increase in the surface temperature.

Because the condensation coefficient and the evaporation coefficient should coincide with each other in the equilibrium state, it can be understood from the balance theorem that the energetic surface molecules can easily escape from the interface. Therefore, only the molecules leaving the liquid−vapor interface were examined. Figure 3 shows the velocity distribution functions for all-leaving, evaporating, and reflecting molecules for the 120 K system. Qualitatively similar results have been obtained at the other temperatures. For the tangential components of velocity V_x and V_y shown in Figure 3a, the three kinds of distribution functions (all-leaving, evaporating, and reflecting molecules) are well consistent with the Maxwellian model. However, some systematic differences are found for the normal component V_z. That is, although the velocity distribution function for all-leaving molecules is well expressed by the Maxwellian model, those for the evaporating and reflecting molecules show deviations. The velocity distribution for the evaporating molecules is larger than the Maxwellian velocity distribution in the large velocity region but smaller in the low-velocity region, whereas the reflecting molecules show an inverse deviation with much difference. This means that the evaporating molecules have larger translational energies than the average described by the Maxwellian velocity distribution, and the reflecting molecules reflect in a way different from that predicted by the Maxwellian model. To put it more precisely, to express the characteristics of evaporation and reflection at the liquid−vapor boundary, the following distribution density functions for the normal velocity component have been proposed in the form of a modified Maxwellian ensemble with the use of eq 1,

TABLE 2: Parameters of the C−C Potential[33] and the SPC/E Potential[35]

parameters	C−C	SPC/E
r_{OH} (Å)	0.9572	1.0
∠HOH (deg)	104.52	109.47
q_{H^+} (C)	0.18559e[a]	0.4238e
$q_{O^{2-}}$ (C)	−0.37118e	−0.8476e

[a] $1e = 1.602\ 177\ 33 \times 10^{-19}$ C.

$$F_{e,z} = \frac{1-\beta\exp[-E_z/(k_B T)]}{1-\beta/2}\left(\frac{m}{k_B T}\right) V_z \exp\left(-\frac{E_z}{k_B T}\right) \quad (3a)$$

$$F_{r,z} = \frac{1-\alpha+\alpha\beta\exp[-E_z/(k_B T)]}{1-\alpha+\alpha\beta/2}\left(\frac{m}{k_B T}\right) V_z \exp\left(-\frac{E_z}{k_B T}\right) \quad (3b)$$

Here, $F_{e,z}$ and $F_{r,z}$ are the distribution densities for the evaporating and reflecting molecules, respectively. Figure 3b includes these distribution density functions, and the comparison shows good agreement with the MD data.

III. Molecular Dynamics Simulation Method

Two kinds of potential models for water, the C−C[33] and the extended simple point charge (SPC/E)[35] interaction potentials, are used in the present simulations. Both models treat the intermolecular interactions via a combination of the short-range pairwise potential of atoms and the long-range Coulombic interaction. A brief comparison of the potential parameters can be found in Table 2, where, r_{OH} is the OH bond length, ∠HOH is the HOH bond angle, and q_{H^+} and $q_{O^{2-}}$ are the charges of the hydrogen and oxygen sites, respectively. For simulations with the SPC/E potential model, the Ewald summation method[36] is used to calculate the Coulombic interactions and bond lengths are constrained using the Shake algorithm.[37] All simulations are performed in NVT ensembles of quasi-equilibrium systems. The Leapfrog method is applied to integrate Newton's equation of motion, with a time step of 0.5 fs. The basic cell is a three-dimensional rectangular enclosure of 32 Å × 32 Å × 192 Å as shown in Figure 4, and a thin liquid film consisting of 1024 water molecules is formed at the central region. Periodic boundary conditions are adopted for all boundaries. The simulation started from an initial arrangement of an fcc lattice, and velocity scaling was applied for each temperature during the first 25 ps. Then, the system is equilibrated for another 25 ps without velocity scaling. The equilibrated system is run for another 110 ps before any analysis is performed. In ref 39 an

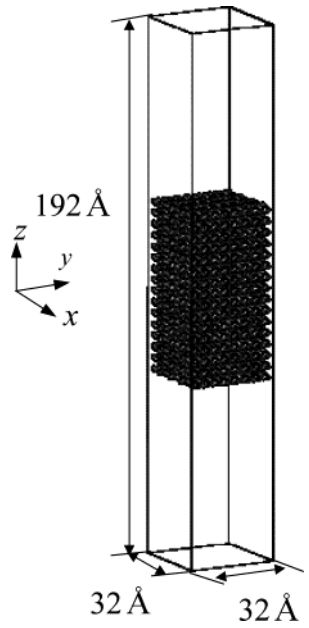

Figure 4. Simulation system. A rectangular section of water in the center is sandwiched between the top and bottom section of vapor. The *z*-axis is perpendicular to the liquid−vapor interface. The initial configuration is an fcc lattice arrangement of water molecules.

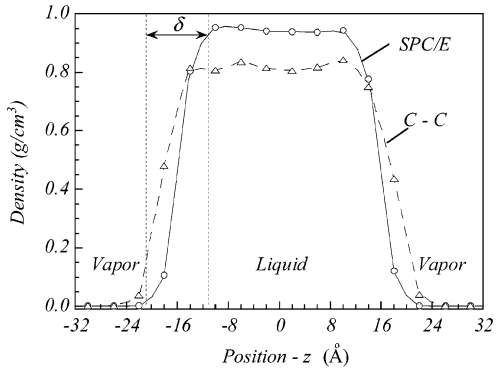

Figure 5. Comparison of the density profiles between the C−C and the SPC/E models at 330 K. The interface thickness δ is defined as the thickness over a region where the bulk vapor changes to bulk liquid (here, it is defined as the thickness over which the density of water changes from $0.95\rho_l$ to $(\rho_g + 0.01\rho_l)$). The lines are guides for the eye.

equilibration period of 125 ps has been used for the SPC/E water interface, and ref 40 suggests that 200 ps is required to reach equilibration for a mixture of DMSO molecules to a pure interface of water. In our simulations the system reached thermal quasi-equilibrium states within 160 ps. Further simulation for data sampling starts from this state.

Figure 5 shows a comparison of the density profiles between the C−C and the SPC/E models at 330 K. The liquid density of the central region is around 0.8 g/cm^3 for the C−C model and 0.96 g/cm^3 for the SPC/E model. Because the 330 K liquid water has a density of 0.98 g/cm^3, it is understood that the C−C potential model gives a smaller liquid density, whereas the SPC/E model shows good agreement with practical data. For simulations at temperatures above 330 K, we only adopted the SPC/E model because of its good correspondence with experimental data.[39] The results for the liquid−vapor coexistence curve at temperatures between 330 and 550 K are plotted in Figure 6. It shows that the MD data of the SPC/E model agree well with the properties of water.

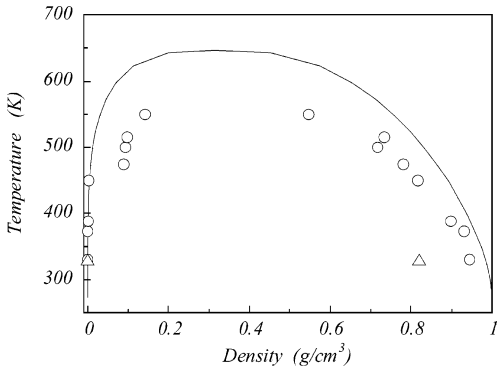

Figure 6. Liquid−vapor coexistence curve. The solid line represents the property of water.[42] Open circles are the MD results using the SPC/E model, and the open triangle corresponds to the C−C model.

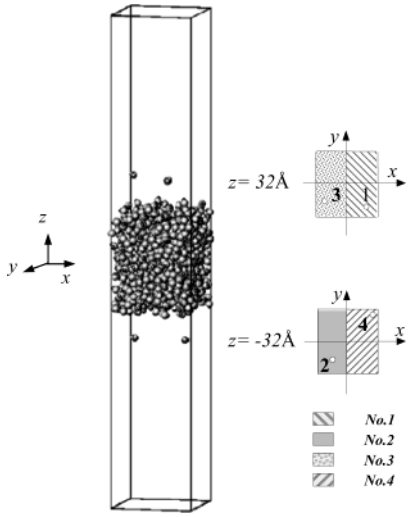

Figure 7. Injecting position of the test molecules. Four molecules are injected for one calculation at the initial position of $z = \pm 32$ Å. The initial positions for *x* and *y* are given randomly within a half area shown.

IV. Results and Discussion

IV.A. Injection Simulations and Molecular Exchange Effect. Injection simulations performed by injecting test molecules onto the liquid film were used to examine the molecular interactions and the molecular exchange effect at the liquid−vapor interface. It is known that the structure and dynamics of the liquid−vapor interface are different for the C−C potential and the SPC/E model. However, how the condensation, evaporation, reflection, or the molecular exchange phenomena are affected by such a difference has not been studied. The earlier study using the C−C model[33] has shown no marked effect of the molecular exchange phenomenon, which is inconsistent with Matsumoto's results.[20] Thus, we expected that the use of the SPC/E model would make a difference to the previous results for the C−C model.

The detailed incident method and conditions are depicted in Figure 7 and Table 3. Two test molecules are injected onto each surface in one calculation. The initial location (*x*, *y*) of each molecule is given randomly within a half area of each surface to exclude mutual interactions of the test molecules. The *z*-position is set at $z = \pm 32$ Å which is outside the potential variation region from the liquid film. Also, the initial orientation of the test molecule is given randomly, and the incident translational energy and rotational energy are given according to the Maxwellian velocity distribution function. The incident angles of 30°, 45°, and 60° are used for comparison with the condition of 0° (i.e., normal to the surface). After one calculation

TABLE 3: Incident Conditions and Condensation Coefficients of Test Molecules[a]

model	C−C										SPC/E				
simulation	A	B	C	D	E	F	G	H	I	J	K	L	M	N	O
E_{tr}[b]	0.60	2.28	9.57	0.60	9.57	12.8	1.20	19.2	2.39	38.3	2.28	2.28	2.28	2.28	2.58
E_z[c]	0.60	2.28	9.57	0.60	9.57	9.57	0.60	9.57	0.60	9.57	2.28	2.28	2.28	2.28	2.58
E_{rot}[d]	0	0	0	0.60	9.57	0	0	0	0	0	0	2.28	6.84	11.4	0
θ (deg)[e]	0	0	0	0	0	30	45	45	60	60	0	0	0	0	0
N_{in}[f]	92	92	96	92	98	96	80	90	76	80	100	100	100	100	100
N_c[g]	86	88	96	85	98	96	74	88	72	78	98	100	98	100	100
N_r[h]	6	4	0	7	0	0	6	2	4	2	2	0	2	0	0
N_{exch}[i]	13	8	6	12	10	16	17	8	15	12	2	5	6	9	10
σ_{c-self}[j]	0.935	0.957	1.000	0.924	1.000	1.000	0.925	0.977	0.947	0.975	0.980	1.000	0.980	1.000	1.000
σ_{c-net}[k]	0.793	0.870	0.938	0.793	0.898	0.833	0.712	0.889	0.750	0.825	0.960	0.950	0.920	0.910	0.900

[a] System temperature is 330 K for cases A−N and 373 K for case O. All energies are in 10^{-21} J per test molecule. [b] Translational energy of the incident molecule. [c] Normal component of the translational energy. [d] Rotational energy of the incident molecule. [e] Incident angle. [f] Number of incident molecules. [g] Number of condensed molecules. [h] Number of reflected molecules. [i] Number of evaporated molecules due to molecular exchange phenomena. [j] Condensation coefficient (self) in eq 4. [k] Condensation coefficient with consideration of the molecular exchange rate (net), see eq 5.

the condition of the liquid film system is set back to the initial equilibrium state, and a new calculation always starts in the same system condition. For one incident condition, 25 calculations are carried out and the data for 100 test molecules are collected.

The condensation coefficient σ_{c-self} is defined as the fraction of condensing molecules N_c to all incident molecules N_{in}:

$$\sigma_{c-self} = \frac{N_c}{N_{in}} \tag{4}$$

The subscript "self" denotes that it is defined as a "self-condensation probability". The condensation coefficient σ_{c-net} is defined as:

$$\sigma_{c-net} = \sigma_{c-self} - \sigma_{exch} = \frac{N_c - N_{exch}}{N_{in}} \tag{5}$$

The subscript "net" denotes a meaning of "net condensation rate", that is, a decrease in rate due to the molecular exchange is introduced to the definition of the condensation coefficient. The results of these two kinds of condensation coefficients are summarized in Table 3. The simulations A−J in Table 3 are results obtained from the C−C model, and the others are from the SPC/E model. Although frequent molecular exchange phenomena were expected for the SPC/E model, it is found that most of the incident molecules condensed to the liquid, and the molecular exchange ratio is small for both of the potential models. Considering the same incident conditions of B and K, we can see that both the self-and net condensation coefficients for the SPC/E model (case K) are larger than those for the C−C model (case B). In other words, the results produce an effect contrary to our intuition that the molecular exchange phenomena shall be enhanced by the strong SPC/E intermolecular interaction. It is thought that the incident molecules are subjected to a stronger interaction from the liquid phase in the case of the SPC/E model. As demonstrated in Figure 8, the translational energy of the test molecule just before collision with the liquid molecules increases from its initial value, and it is found that the acceleration rate for the case of the SPC/E model (case K with the filled circle) is larger than in the C−C model (case B with the open circle). This is closely related to the fact that the density of the SPC/E liquid film is larger than that of the C−C liquid film, which results in the larger incident energy of the SPC/E molecules. The strong interaction at the interface also confines the surface molecules and makes it difficult to escape

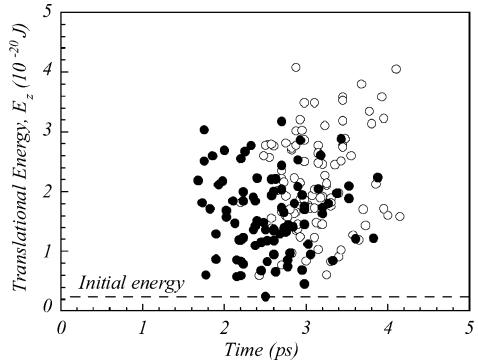

Figure 8. Translational energy just before collision with surface molecules. Open circles correspond to case K in Table 3 for the SPC/E model and filled circles to case B for the C−C model.

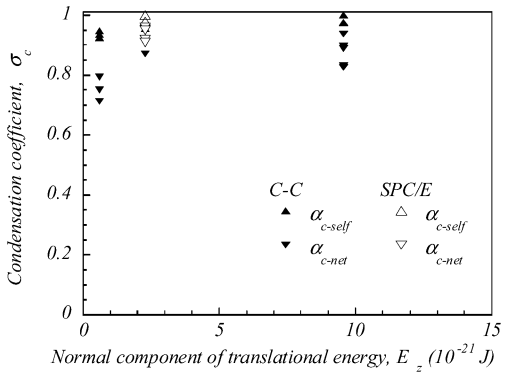

Figure 9. Effects of molecular exchange on condensation coefficients. The results are obtained by injection simulations with the system temperature at 330 K. α_{c-self} is defined in eq 4 and α_{c-net} is defined in eq 5.

from the interface. That is, the large potential energy of water accelerates the vapor molecules to be condensed and reduces the molecular exchange rate, which results in the increase of the condensation coefficient.

The dependency of the condensation coefficient on the kinetic conditions of the incident molecules is depicted in Figure 9 as a function of the normal component of translational energy. It is found that the self-condensation coefficient and the net condensation coefficient increase with the translational energy of the incident molecule in a way similar to that which occurs for argon. However, its value is close to unity and the dependency is small at 330 K. On the other hand, the changes of the incident angle (corresponding to the changes of the

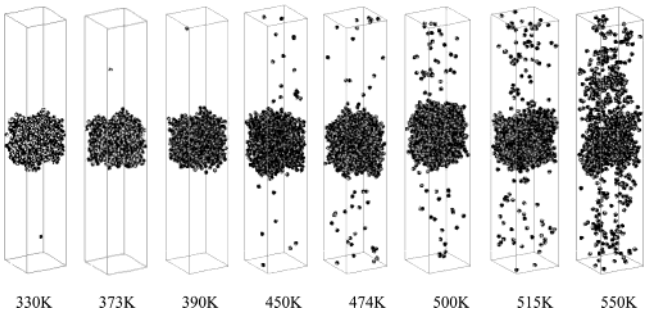

Figure 10. Snapshots of the liquid film in equilibrium situations.

tangential components of the translational energy) and the rotational energy have no marked effect on the condensation coefficients. Comparing cases A and G, or cases C, F, H, and J, we can find that the influence on the incident angle is insignificant. Also, the effect of the rotational energy is examined from cases D, E, and L (the rotational energy is equal to the translational energy), and cases M and N (the rotational energy is larger than the translational energy). The results show a small increase of molecular exchange but no significant effect of rotational energy on the condensation coefficient. This is also seen in the comparison between the cases A and D.

Consequently, the condensation coefficient of water at 330 K is close to unity and the molecular exchange phenomena are insignificant. The different potential models have no marked effect on the condensation coefficients and the molecular exchange rate.

IV.B. Condensation Coefficient at Higher Temperatures. Figure 10 shows snapshots of the systems at temperatures ranging from 373 to 550 K. For simulation systems at temperatures between 450 and 550 K, molecular evaporation from the liquid film becomes frequent and the number density of the vapor increases. Hence, we can acquire information on condensation and evaporation without injecting any test molecules. The condensation coefficient can be calculated by counting the molecular flux adjacent to the interface. The data are collected from the equilibrium state described in section IV.A. for a period of 140 ps. The details of the data sampling are similar to those for argon described elsewhere.[26]

On the basis of the transient recordings on the fluxes of molecules approaching and leaving the interface, mass fluxes for condensation, reflection, and evaporation are separated, and the condensation coefficient is available in accordance with the definition of eq 4. Figure 11 shows the condensation coefficients for SPC/E water as a function of the surface-normal component of the translational energy. By comparison with Figure 2a, we can see condensation characteristics similar to those of argon. That is, the condensation coefficients of water increase with an increase in the surface-normal component of the translational energy and decrease with increase in the surface temperature. This indicates that the high-energy molecules condense easily to a surface that has a higher number density of liquid; in other words, the molecular condensation probability depends on both the molecular incident motion and the condition of the liquid phase. Therefore, it is reasonable to suppose that the condensation coefficient for water can be expressed by eq 1 too, which is proposed by the MD results for argon. Again,

$$\sigma_c = \alpha\left[1 - \beta \exp\left(-\frac{E_z}{k_B T}\right)\right] \qquad (1)$$

The values of the parameters α and β for water are listed in Table 4 and the corresponding results of eq 1 are drawn in Figure 11 with solid lines. We can see that the MD results agree well with the lines. Also, by applying the Maxwellian distribution under equilibrium conditions, the average value of the condensation coefficient is available, and the results are shown in Table 4 and Figure 12.

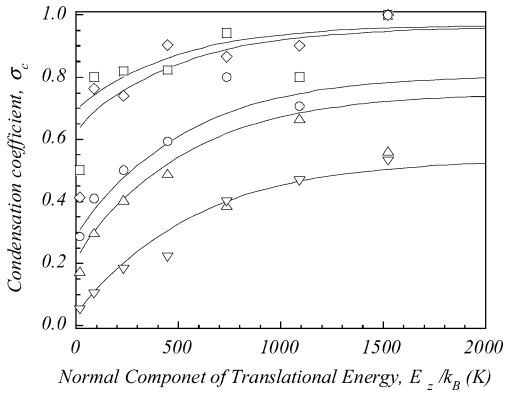

Figure 11. Condensation coefficients and translational energy. Squares correspond to the system temperature of 450 K, diamonds to 474 K, circles to 500 K, triangles (up) to 515 K, and triangles (down) to 550 K. The solid lines show the results from eq 1, and the parameters for water are listed in Table 4 for those corresponding temperatures.

TABLE 4: Parameters and the Mean Value of the Condensation Coefficients[a]

T (K)	α	β	$\bar{\sigma}_c$
330	0.990	0.058	0.961
450	0.967	0.280	0.832
474	0.961	0.337	0.799
500	0.808	0.640	0.549
515	0.750	0.650	0.487
550	0.536	0.932	0.286

[a] T is the temperature of the system; α and β are parameters of the condensation coefficient in eq 1.

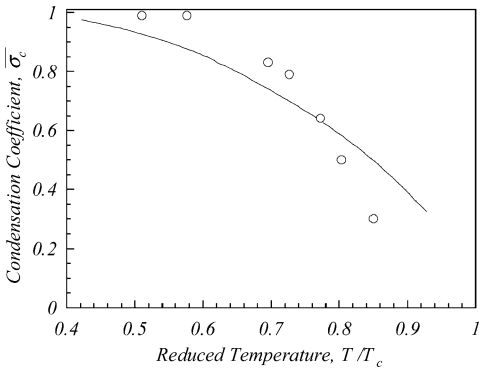

Figure 12. Comparison of the condensation coefficients between transition state theory and molecular dynamics simulation. The temperature shown in the x-axis is reduced by the critical temperature of water (T_c = 647.13 K). Open circles correspond to the MD data and the solid line corresponds to eq 10.

Because the motion of water consists of rotation as well as translation, the effect of rotational energy on the condensation coefficient was examined. On the basis of their theoretical consideration, Fujikawa and Maerefat suggested that the small condensation coefficient of polyatomic vapor is due to the effect of rotational motion.[9] However, inconsistent with their opinion, the effect of the rotational energy is not so significant compared with that of the translational energy in the present work. Thus, we conclude that the translational motion is of primary importance in the condensation of water, and the condensation

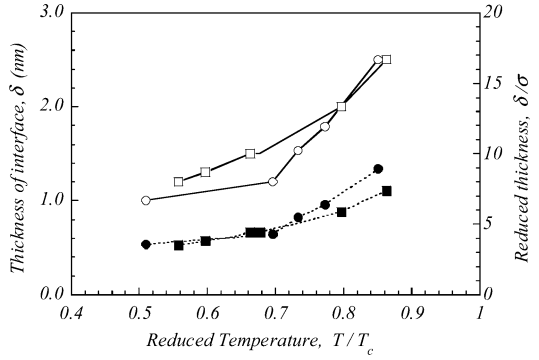

Figure 13. Thickness of the liquid−vapor interface. The interface thickness δ is defined as the thickness over a region where the bulk vapor changes to bulk liquid as shown in Figure 5, which is different from the 10−90 thickness.[38,39,41] The right *y*-axis shows the value reduced by the molecular diameter of argon and water, respectively. Circles correspond to water and squares to argon. The solid lines are guides for the eye for the left *y*-axis (open symbols), and the dotted lines are guides for the eye for the right *y*-axis (filled symbols).

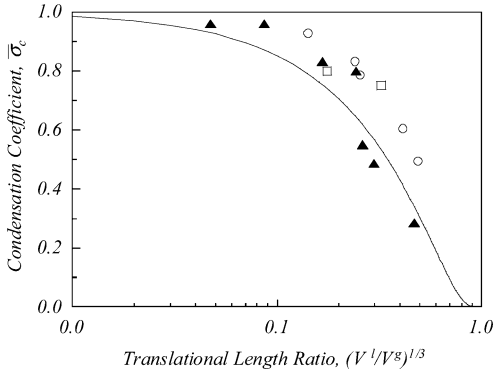

Figure 14. Condensation coefficients as a function of translational length ratio. The solid line corresponds to eq 10 and all symbols are MD data: open circles are for argon (ref 26), filled triangles are for water in the present work, and open squares are for methanol (ref 16).

coefficient depends on the surface-normal component of the translational energy and surface temperature in a way similar to that of a simple gas such as argon.

IV.C. Liquid−Vapor Interface Structure and Condensation Coefficient. As shown in Figure 5, there is a transition region of the interface between the liquid and the vapor phase. In agreement with the previous publications,[38,39,41] the density varies continuously in the interface region. It is known that in the condensation process the incident molecule should lose its translational energy in order to be condensed during the collision with liquid molecules in this region. For the interface at low temperature near the triple point, the interface region is thin and the transition from vapor to liquid occurs sharply. At higher temperatures the thickness of the interface region increases, and the density difference between liquid and vapor reduces. A comparison of the thickness of the liquid−vapor interface for water and argon is plotted in Figure 13, as a function of the surface temperature reduced by the corresponding critical temperature. The interface thickness δ is defined as the thickness over a region where the bulk vapor changes to bulk liquid; here, it is the thickness over which the density of water changes from $0.95\rho_l$ to $(\rho_g + 0.01\rho_l)$ according to the density profiles. The unit of the left axis is Å, and the right axis shows the dimensionless thickness reduced by the molecular diameter. We can see that the interface thickness for water increases with increasing reduced temperature, from 10 to 25 Å, and a similar tendency can be found in the case of argon. This finite length scale gives physical evidence of a three-dimensional structure for the liquid−vapor interface in the form of a kind of interfacial resistance. Because of the inhomogeneous potential field at the interface region, the freedom of translation is constrained during the phase transition from vapor to liquid. The position where the constraint occurs is near the vapor side at low temperatures; however, it turns into the middle of the interface region for the interface at high temperatures. Therefore, although the thickness of the liquid−vapor interface has been ignored in the expression of the interface mass transfer, it plays an important role in the evaluation of the molecular condensation probability. A novel theoretical expression for the condensation coefficient shows that the small value of the condensation coefficient is the result of the constraint of molecular translation.[31,32] That is,

$$\bar{\sigma}_c = \frac{V^*}{V^g}\exp\left(-\frac{E_0}{k_B T}\right) \tag{6}$$

where V^*/V^g is the free volume ratio of the activated complex to the gas, E_0 is the activation energy of condensation, k_B is the Boltzmann constant, and T is the surface temperature. As reported in our previous study,[32] the free volume ratio for a flat interface in equilibrium is evaluated by

$$\frac{V^*}{V^g} = 1 - \sqrt[3]{V^l/V^g} \tag{7}$$

and the activation energy is approximated by

$$E_0 = \left[\frac{4-\beta}{2(2-\beta)} - 1\right]k_B T \tag{8}$$

based on the MD results. Then, the parameters α and β can be derived from the combination of eq 6 with eq 1 as

$$\alpha = \exp\left(-\frac{E_0}{k_B T}\right), \quad \beta = 2\sqrt[3]{V^l/V^g} \tag{9}$$

Consequently, the theoretical formulation of eq 6 becomes

$$\bar{\sigma}_c = (1 - \sqrt[3]{V^l/V^g})\exp\left(-\frac{1}{2}\frac{1}{\sqrt[3]{V^g/V^l} - 1}\right) \tag{10}$$

Comparisons of the computational data and the theoretical results for the condensation coefficients of water are also shown in Figure 12 as a function of the surface temperature, and we can see that the MD data agree very well with the theoretical results. In the theoretical expression of the condensation coefficient of eq 10, the translational length ratio $\sqrt[3]{V^g/V^l}$ is a meaningful factor which implies that the molecular translational motion is restricted at the transition state. It reveals that the nature of condensation is directly related to the molecular motion of liquid and vapor, and that for a given pure liquid−vapor interface, the condensation coefficient is an inherent property. Figure 14 demonstrates the computational data for several substances in comparison with the theoretical prediction, as a function of the translational length ratio in relative agreements.

There is still a discrepancy between our simulations and the experiments for the condensation coefficient of water. An important fact that should be noted is that impurity effects exist in the experimental estimation of the condensation coefficient, whereas the MD simulation has been conducted in an entirely pure system. The experimental data in Figure 1 were measured under pressures lower than one atmosphere, so we should be careful about the invasion of noncondensable gas into the experimental measuring system. The existence of small amounts

of noncondensable gas in the system may reduce the measured value of the condensation coefficient, because of its accumulation at the condensation interface. This problem deserves attention and further exploration in order to explain the discrepancy of the condensation coefficients between simulations and experiments.

V. Conclusions

The molecular condensation behavior of water at the liquid−vapor interface has been studied using molecular dynamics simulations. The effects of the molecular exchange phenomena and the translational and rotational energies on the condensation coefficient are examined and the following conclusions have been derived:

1. The molecular exchange phenomena have an insignificant effect on the condensation coefficient.

2. Equation 1 presents a microscopic boundary condition for the evaluation of condensation for both monatomic and polyatomic molecules. The condensation coefficient of water depends on the normal component of the molecular incident translational energy and the surface temperature in a way similar to that of argon.

3. The translational motion is of primary importance to the condensation process, whereas the effect of the rotational motion is insignificant. The small value of the condensation coefficient is due to the constraint of translational motion at the liquid−vapor interface within the three-dimensional structure. The MD data are in good agreement with the theoretical prediction of eq 10.

Acknowledgment. This work was supported by the Ministry of Education, Science, and Culture of the Japanese Government through the Grant-in-Aid for Scientific Research (c), Project No. 06650259.

References and Notes

(1) Marek, R.; Straub, J. *Int. J. Heat Mass Transfer* **2001**, *44*, 39.
(2) Mozurkewich, M. *Aerosol Sci. Technol.* **1986**, *5*, 223.
(3) Eames, I. W.; Marr, N. J.; Sabir, H. *Int. J. Heat Mass Transfer* **1997**, *40*, 2963.
(4) Mills, A. F.; Seban, R. A. *Int. J. Heat Mass Transfer* **1967**, *10*, 1815.
(5) Maa, J. R. *Ind. Eng. Chem. Fundam.* **1969**, *8*, 564.
(6) Wenzel, H. *Int. J. Heat Mass Transfer* **1969**, *12*, 125.
(7) Bonacci, J. C.; Myers, A. L.; Nongbri, G.; Eagleton, L. C. *Chem. Eng. Sci.* **197**6, *31*, 609.
(8) Hatamiya, S.; Tanaka, H. *Proc. Int. Heat Transf. Conf., 8th* **1986**, *4*, 1671.
(9) Fujikawa, S.; Maerefat, M. *Trans. Jpn. Soc. Mech. Eng., B* **1990**, *56*, 1376.
(10) Maerefat, M.; Akamatsu, T.; Fujikawa, S. *Exp. Fluids* **1990**, *9*, 345.
(11) Tsuruta, T.; Masuoka, T.; Kato, Y. *Therm. Sci. Eng.* **1994**, *2*, 98.
(12) Kincaid, J. F.; Eyring, H. *J. Chem. Phys.* **1938**, *6*, 620.
(13) Matsumoto, M.; Kataoka, Y. *J. Chem. Phys.* **1989**, *90*, 2398.
(14) Yasuoka, M.; Matsumoto, K.; Kataoka, Y. *J. Mol. Liq.* **1995**, *65*, 329.
(15) Yasuoka, K.; Matsumoto, M.; Kataoka, Y. *J. Chem. Phys.* **1994**, *101*, 7904.
(16) Matsumoto, M.; Yasuoka, K.; Kataoka, Y. *J. Chem. Phys.* **1994**, *101*, 7912.
(17) Matsumoto, M.; Yasuoka, K.; Kataoka, Y. *Fluid Phase Equilib.* **1995**, *104*, 431.
(18) Yasuoka, M.; Matsumoto, K.; Kataoka, Y. *J. Mol. Liq.* **1995**, *65*, 329.
(19) Matsumoto, M. *Mol. Simul.* **1996**, *16*, 209.
(20) Matsumoto, M. *Fluid Phase Equilib.* **1998**, *144*, 307.
(21) Fujikawa, S.; Matsumoto, M.; Kotani, M.; Sato, H. *Trans. Jpn. Soc. Mech. Eng.* **1995**, *61*, 215.
(22) Matsumoto, M.; Fujikawa, S. *Microscale Thermophys. Eng.* **1997**, *1*, 119.
(23) Chekmarev, S. F. *AIChE J.* **1996**, *42*, 2467.
(24) Meland, R. *J. Chem. Phys.* **2002**, *117*, 7254.
(25) Tsuruta, T.; Sakamoto, N.; Masuoka, T. *Therm. Sci. Eng.* **1995**, *3*, 85.
(26) Tsuruta, T.; Tanaka, H.; Masuoka, T. *Int. J. Heat Mass Transfer* **1999**, *42*, 4107.
(27) Tsuruta, T.; Tanaka, H.; Tamashima, K.; Masuoka, T. *Trans. Jpn. Soc. Mech. Eng., B* **1997**, *63*, 2776.
(28) Tsuruta, T.; Tanaka, H.; Masuoka, T. *Trans. Jpn. Soc. Mech. Eng., B* **1998**, *64*, 456.
(29) Kjelstrup, S.; Tsuruta, T.; Bedeaux, D. *J. Colloid Interface Sci.* **2002**, *256*, 451.
(30) Tsuruta, T.; Nagayama, G. *Therm. Sci. Eng.* **2002**, *10*, 9.
(31) Nagayama, G.; Tsuruta, T. *Trans. Jpn. Soc. Mech. Eng., B* **2001**, *67*, 183.
(32) Nagayama, G.; Tsuruta, T. *J. Chem. Phys.* **2003**, *118*, 1392.
(33) Carravetta, V.; Clementi, E. *J. Chem. Phys.* **1984**, *81*, 2646.
(34) Tsuruta, T.; Fukumoto, H.; Nagayama, G.; Masuoka, T. *Proc. ASME−JSME Therm. Eng. Jt. Conf., 5th* **1999**, *AJTE99−6509*, 1.
(35) Berendsen, H. J. C.; Grigera, J. R.; Straatsma, T. P. *J. Phys. Chem.* **1987**, *91*, 6269.
(36) Allen, M. P.; Tildesley, D. J. *Computer Simulation of Liquids*; Oxford University Press: New York, 1987.
(37) Ryckaert, J. P.; Ciccotti, G.; Berendsen, H. J. C. *J. Comput. Phys.* **1977**, *23*, 327.
(38) Matsumoto, M.; Kataoka, Y. *J. Chem. Phys.* **1988**, *88*, 3233.
(39) Alejandre, J.; Tildesley, D. J.; Chapela, G. A. *J. Chem. Phys.* **1995**, *102*, 4574.
(40) Benjamin, I. *J. Chem. Phys.* **1999**, *110*, 8070.
(41) Taylor, R. S.; Dang, L. X.; Garrett, B. C. *J. Phys. Chem.* **1996**, *100*, 11720.
(42) Schmidt, E. *Properties of Water and Steam in SI-Units*; Springer-Verlag: Berlin, 1969.